Proceedings of the ASME 2023 42nd International Conference on Ocean, Offshore and Arctic Engineering
OMAE2023
June 11–16, 2023, Melbourne, Australia

OMAE2023-108101

ULTRASONIC WELL INTEGRITY LOGGING USING PHASED ARRAY TECHNOLOGY

Tonni Franke Johansen[1,2,*], Philip Erik Buschmann[1], Knut Marius Røsberg[1], Anja Diez[1], Erlend Magnus Viggen[2]

[1]SINTEF Digital, Trondheim, Norway
[2]Norwegian University of Science and Technology, Trondheim, Norway

ABSTRACT

Ultrasonic well integrity logging is an important and common procedure for well completion and plug-and-abandonment operations. Typical logging tools employ single-element ultrasound transducers. In medical ultrasound imaging, however, more flexible phased arrays are the standard. This paper presents a first set of experimental results obtained with up to two linear 32-element phased arrays that are specifically designed for plug-and-abandonment operations in terms of their centre frequency. The experiments encompass pulse-echo and pitch-catch studies for different incidence angles and aperture sizes on plates and pipes with wall thickness as encountered in the offshore industry. The pulse-echo experiment is backed up by simulations, and shows that effect of the incidence angle on the pipe resonance's frequency and strength is weak and more strong, respectively, and that the effect depends on the frequency response and directivity of the transducer. The pitch-catch experiment demonstrates the importance of carefully choosing the right angle of incidence to excite the intended wave modes.

Keywords: Ultrasound, Phased arrays, Oil well integrity, Plug and Abandonment, Guided waves, Pulse echo, Pitch catch

1. INTRODUCTION

Ultrasonic well logging is a prevalent method used by offshore service companies to obtain data from boreholes. The method uses a probe containing one or more single element ultrasound transducers. Here, 'single element' refers to transducers with only one active element. In cased-hole logging, waves are typically transmitted through the borehole fluid into the surrounding pipe and the responses are recorded [1–5]. The obtained signals can be used to reconstruct the pipe thickness, if any damage has occurred to the pipes by drill bits, and whether cement is sufficiently bonded to the outside of the innermost pipe. The measurements can cover the full borehole by rotating the probe as it moves up and out of the borehole. Thus, ultrasonic cased-hole logging can identify structural deficiencies so that countermeasures can be implemented. In this paper, phased arrays are employed to record more data than is available from common ultrasonic well logging setups.

Ultrasound has many advantageous properties. It is non-destructive, works in corrosive environments, permits finding subsurface features and works on metallic components [6]. However, the interpretation of ultrasound signals becomes difficult in complex geometries due to the manifold scattering of the waves on boundaries. This is one reason why current applications inside of oil wells only employ a few transducers in *pulse–echo* (PE) or *pitch–catch* (PC) mode (Fig. 1a). In PE mode, a transducer transmits a wave straight onto the pipe wall and records the echo. In PC mode, a wave is transmitted at an angle onto the pipe wall, exciting guided waves in the pipe wall. These waves travel along the pipe wall while emitting wavefronts that are recorded at a 2nd and/or 3rd transducer. In practical applications, the data is processed on the device, compressed, and transmitted out of the borehole. The bandwidth between the tool and the surface is relatively low [7]. This is another reason why solutions with more sensors cannot be readily implemented.

In contrast, the field of medical ultrasound imaging has for decades mainly employed phased arrays to perform imaging of the human body for diagnostic [8] and therapeutic [9, 10] purposes. Phased arrays consist of a large number of piezoceramic elements that act as individual transducers. By using multi-channel fast electronics, these elements are excited individually. This permits steering and focusing an ultrasonic beam without mechanically moving the array. Such a control of the transmitted ultrasonic wave is achieved by prescribing delays [11] between the excitation of the individual elements to direct the converging wavefront into specific directions or onto specific points. In medical diagnostics, generally between 128 and 512 elements are employed in a linear, curved or matrix-style arrangement. Moreover, signals are collected on all channels simultaneously, which yields a large amount of data that can be combined via beamforming [12] to

*Corresponding author: tonni.f.johansen@sintef.no

Author Accepted Manuscript version of the paper by Johansen et al. in Proceedings of the ASME 42nd International Conference on Ocean, Offshore and Arctic Engineering, Vol. 9 (2023), DOI:10.1115/OMAE2023-108101

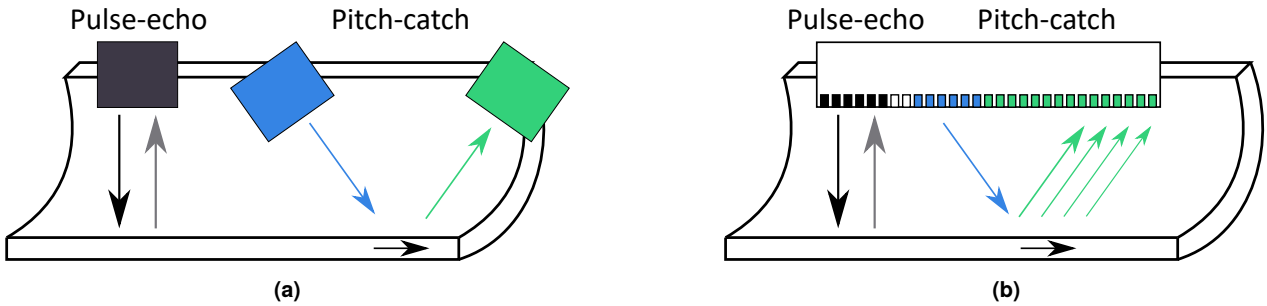

FIGURE 1: A) A SETUP WITH THREE SINGLE ELEMENT TRANSDUCERS TO EVALUATE A PIPE IN PULSE-ECHO AND PITCH-CATCH MODE. B) AN ULTRASOUND ARRAY WITH A NUMBER OF ACTIVE ELEMENTS CAN OPERATE IN BOTH MODES BY ELECTRONICALLY STEERING GROUPS OF ELEMENTS, HERE IDENTIFIED BY THE SAME COLOURS AS IN A).

create images. A large amount of literature on imaging techniques exists for medical applications [8, 13] and non-destructive testing (NDT) [14–16].

Phased array technology can be an asset for ultrasonic inspections in oil wells. The high bandwidth necessary to operate them on an actual probe inside an oil well bars them from an immediate application — for now. However, the rapid parallel data acquisition with minimal mechanical movement makes them attractive for testing new solutions. Phased arrays can be operated in PE and PC mode, just like a set of single element transducers (Fig. 1b). In this manner, the large number of channels yields significantly more information than would be available from single element transducers. This can be exploited to design better signal processing algorithms for existing ultrasound logging tools or to validate numerical simulations. In the long term, phased arrays may allow imaging methods that yield higher resolution and allow to identify structural defects better.

This paper presents a set of first results where phased arrays are used in an experimental laboratory. This ultrasound laboratory is part of a larger Norwegian initiative [17] with several facilities that all develop technologies for the plug and abandonment [18, 19] of oil wells. The core component in this laboratory are phased arrays with a centre frequency of 240 kHz that can be operated under moderate pressure. The target bandwidth of the array is 185 – 315 kHz, so it can be used with a range of pipe thicknesses (9 – 14 mm). No off-the-shelf product is available and, hence, a set of first prototypes are used in this study. As the arrays are prototypes, significant testing is necessary to ensure a satisfactory performance. Therefore, this paper first presents results on a simple flat plate where the arrays are employed in PE and PC mode — replicating the current application in industrial devices. The results are compared to numerical simulations of single-element transducers. This is followed by a first result on a setup with two concentric pipes that is a model of a pipe layout inside a borehole (Fig. 3b). The arrays are placed inside of the innermost pipe and mechanically moved along the pipe to record a PC measurement for the entire length of the setup.

One aim with the laboratory is to develop technology to evaluate cement bonding on the interface outside of the second pipe — a capability that is important for cost-effective plug and abandonment of oil wells. While complete realisations of this capability have not yet been shown, the literature covers various experimental studies [5, 20, 21], limited theoretical methods [22–25], and a practical heuristic method giving estimates via machine learning [26]. The laboratory also allows measuring the sound field outside of the concentric pipes. This feature in combination with the flexibility of phased arrays is expected to be highly beneficial for solving this difficult problem at a later stage.

This paper is structured as follows: In Section 2 a description of the ultrasound arrays, the experiments and a numerical setup are given. Section 3 collects the results for the simple experiment with a flat plate and Sec. 3.3 gives a brief outlook into the more complex experiment with concentric pipes. The conclusion in Sec. 4 summarises the results and presents an outlook into future work.

2. EXPERIMENTAL AND NUMERICAL SETUP

In this section, the employed custom linear arrays are presented and the two considered experiments are described. Moreover, details of the numerical setup that is employed for comparison are given.

2.1 Ultrasound arrays and instrumentation

Ultrasound signals are transmitted and received by using two custom linear arrays. Each array consists of 32 elements with a pitch of 3 mm (Fig. 2a). Each element has a transverse (elevation) width of $T = 25$ mm. The first prototype arrays have a centre frequency $f_c = 240$ kHz and bandwidth of 40% (−6 dB, 180 − 280 kHz), and there are variations in the sensitivities between elements. Therefore, the arrays have some shortcomings in exciting the mode with a resonance of 290 kHz for a steel pipe with thickness 10.0 mm. This is one motivation to employ the arrays on a flat plate of thickness 12.1 mm as detailed later.

The arrays are controlled with a research ultrasound scanner from the company Verasonics. The model is called Vantage 128 and is in the low frequency configuration, optimised for the 50–1500 kHz range. A simple tri-state pulse of frequency f_c with two half cycles and duration of 0.67 of a full period is used to excite the individual elements. Steering angles α of the beam are realised by prescribing suitable delays between element excitations. The data is saved at a sample frequency of $f_s = 12.5$ MHz following a prior decimation by a factor of 5 of the raw data after the A/D conversion. Two digital lowpass filters are applied to the data:

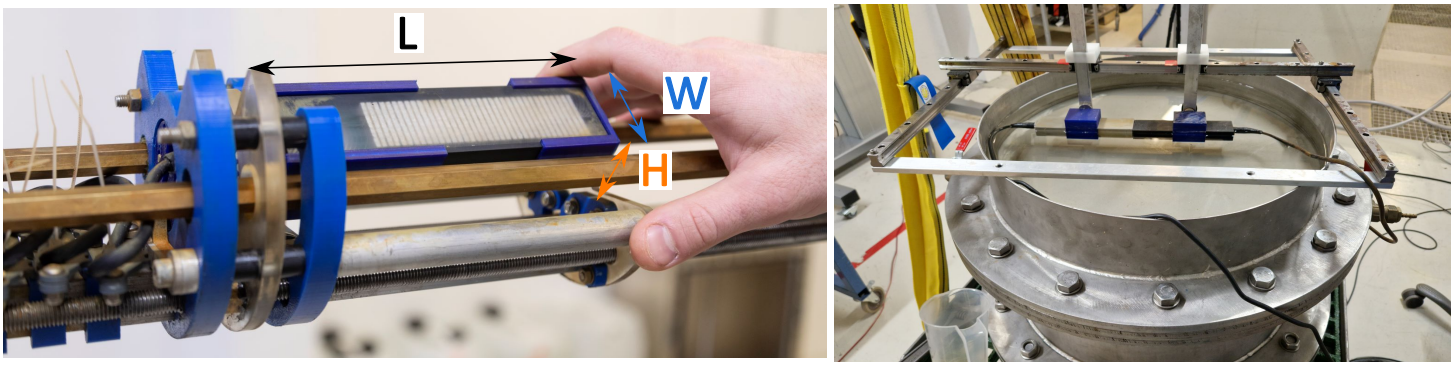

(a) (b)

FIGURE 2: A) PHOTO OF THE EMPLOYED CUSTOM ARRAYS MOUNTED INSIDE OF THE TRAVERSE SYSTEM. THE INDIVIDUAL ELEMENTS ARE VISIBLE AS WHITE STRIPS. THE OUTER DIMENSIONS OF THE ARRAYS ARE $L = 154\,\text{mm}$, $W = 38\,\text{mm}$ AND $H = 25\,\text{mm}$. B) EXPERIMENT WITH A STEEL DRUM WHERE THE TWO ARRAYS ARE PLACED PARALLEL TO THE PLATE.

one with corner frequency 10 MHz prior to the decimation and another with 1 MHz before saving. Each recording consists of the data from every channel and $8 \cdot 10^3$ samples. No apodisation is employed during the recording.

2.2 Experimental setups

Two experimental setups are considered in this work: a simplified setup with a flat plate and a setup with concentric pipes. Henceforth, we will refer to the former as the 'steel drum experiment' and the latter as the 'pipe experiment'.

The steel drum experiment is depicted in Fig. 2b; this drum setup was previously investigated by [21]. A circular top basin of diameter 500 mm is filled with water and the arrays are placed parallel at a distance of 50 mm to the bottom steel plate. The bottom plate is of thickness 12.1 mm and is the target of the investigation. A cavity below the steel plate can be filled with an arbitrary fluid and pressurised up to 2.2 bars to study the effect on the observed ultrasonic waves. In this study, only air and water at ambient pressure are used. To avoid undesired air bubbles forming in the water on the backside of the measurement surface, the lower cavity is first filled with water and left standing for 24 h. During this time small air bubbles form on the steel surfaces which are then wiped off. Afterwards, the cavity is filled to the brim with water again (only a small amount necessary due to spillage while wiping) and closed while a small valve is left open in the flat plate, which serves as the lid. As the setup is tightened, air and water escape through the valve. After the flat plate has been tightened to the filled cavity, the valve is closed off. The ultrasonic arrays are mounted on a rail where they can be moved axially with respect to each other and remain parallel with respect to the steel target. Similarly, the top cavity is filled with water and it is ensured that no air bubbles are obstructing the paths of the ultrasonic waves.

A pulse-echo experiment was performed to simulate tilting of a single element probe, imitating how probe eccentering in a pipe causes angled beam incidence. Beams were transmitted with angles of incidence α from $-10°$ to $10°$, with steps of $1°$, from apertures of 4 elements (12 mm) and 8 elements (24 mm). Echo waveforms were recorded for all 32 elements for post processing. The first step of the post processing was to beamform by applying the transmit tilt on the received data and average over the receive aperture, which was the same as the transmit aperture.

A pitch-catch experiment was performed to investigate excitation of leaky Lamb waves in the plate as function of angle of incidence. For this case, one array was used for transmitting and another for recording waveforms at two positions. The distance between the transmitting aperture, which was 8 elements wide, was 42 mm and 99 mm. The transmit beams were tilted at several angles.

The pipe experiment is depicted in its assembled form in Fig. 3b. The experiment consists of two 2 m long pipes that are arranged concentrically. The inner pipe has a diameter of 177.80 mm (7 in) and the outer pipe 244.48 mm (95/8 in). Their thicknesses are 10.0 mm (0.433 in) and 13.8 mm (0.543 in), respectively. These diameters and thicknesses are chosen to represent segments of standard pipes in use in the oil industry. Both the inner and the outer cavities are filled with water. In principle, both cavities can be filled with other substances but this is not conducted here. The arrays are placed onto movable sleds inside of the inner pipe, with the left sled depicted in Fig. 3a. When mounted inside the pipe, the array surface is 50 mm from the inner pipe wall. Figure 3b shows this part of the setup mounted onto the left hand side. The positions are controlled via a computer program and coupled to the recording software to permit a fast acquisition process. Three movements are possible: axial, circumferential, and a tilting of the arrays to deviate from the normal direction. Separate axial and tilting positions can be prescribed for the two arrays but only one circumferential position for both. The entire setup can be submerged into a water tank to permit acoustic measurements from the outside.

In order to demonstrate the functionality of the system, a PC experiment is conducted in the pipe experiment shown in Fig. 3b and the result is depicted in Fig. 7. Hereby the left array is kept fixed and transmits at an angle of $30°$ onto the inner pipe wall with an aperture of 8 elements. The aperture is chosen to guarantee that the steering angle of $30°$ can be realised [27] with the given centre frequency and element pitch. The angle is chosen according to a computation with a dispersion calculator

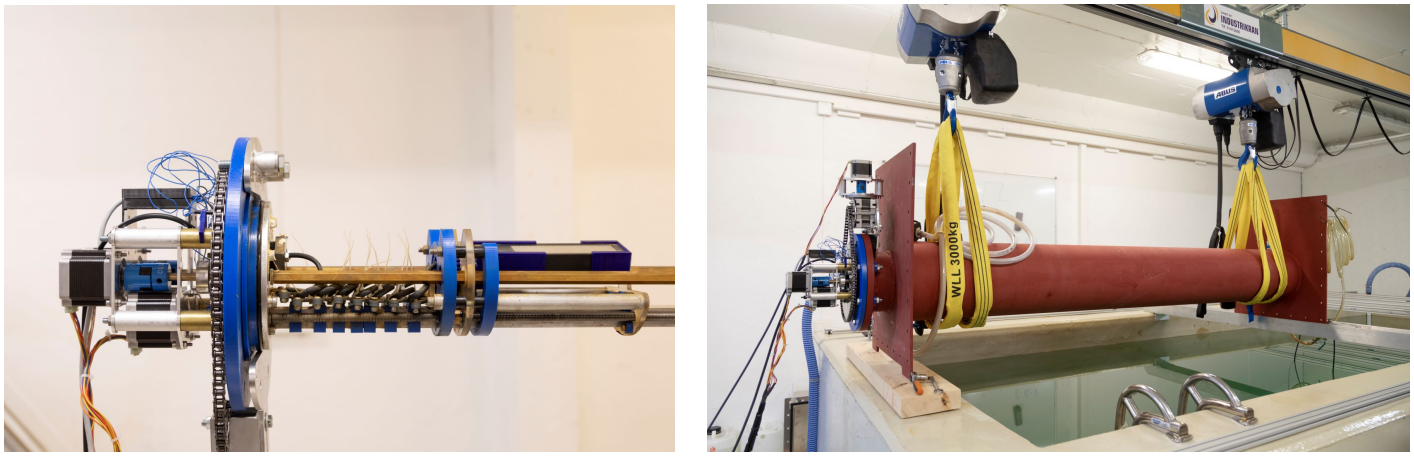

(a) (b)

FIGURE 3: PICTURES OF THE EXPERIMENTAL SETUP WITH CONCENTRIC PIPES. A) ULTRASOUND ARRAY MOUNTED ONTO A THE TRAVERSE SYSTEM. THE STEPPER MOTORS ON THE LEFT REALISE THE MOVEMENT INSIDE OF THE INNER PIPE IN AXIAL, CIRCUMFERENTIAL AND TANGENTIAL DIRECTION. B) THE ASSEMBLED SETUP WITH THE POSITIONING SYSTEM MOUNTED ON THE INSIDE. THE ENTIRE SETUP CAN BE SUBMERGED TO PERMIT MEASUREMENTS FROM THE OUTSIDE (NOT CONDUCTED IN THIS PAPER).

[28] to excite the A_0 and S_0 mode. The right array is placed immediately next to the array and moved in steps of 96 mm and ten times to cover the entire length of the pipe in a non-overlapping fashion. At every position, a recording is conducted. In order to minimise the detrimental effect of possible air bubbles, the setup is rotated such that the arrays are facing downwards, since it is expected that small leakages cause an accumulation of air bubbles on the innermost pipe wall in top. The entire recording takes approx. 3 min, which is almost entirely due to the movement of the recording array by the stepper motors.

2.3 Numerical setup

Simulations were carried out in COMSOL Multiphysics using the time-explicit formulation in 3D. The model is shown in Figure 4a, using a coupling between the pressure acoustics domain (grey) and the elastic wave domain (blue). The transducer has an aperture of 25 mm and emits a Gaussian pulse with a frequency of 250 kHz. A sine apodisation has been employed to taper effects from the edge of the transducer when sending the pulse. We make use of one symmetry axis to reduce the size of the model. The model domain is surrounded by an absorbing layer to suppress edge reflections, thus modelling an infinitely large plate. The plate can be tilted relative to the transducer. Figure 4b shows a snapshot at 70 µs of the model with air behind the pipe, which is modelled approximately by using a free boundary. The model is run for 140 µs and the pressure is averaged over the transducer face to obtain the received time signal.

3. RESULTS AND DISCUSSION

This section presents and discusses the experimental results. First, we cover the pulse echo experiment on a plate, which we compare with the simulation results. Next, we cover the two pitch catch experiments.

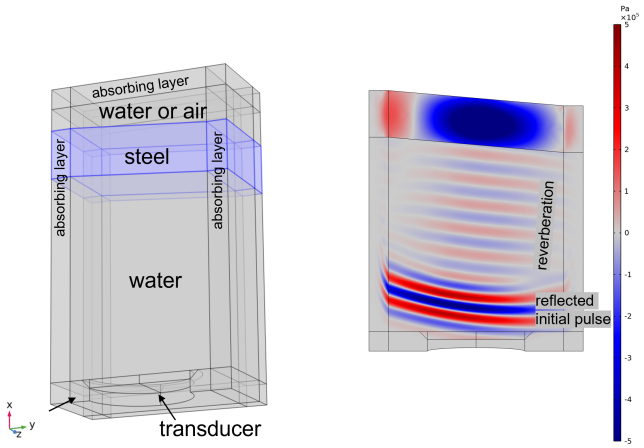

(a) (b)

FIGURE 4: A) COMSOL MODEL SETUP, HERE SHOWN WITH A 5° TILT. B) RESULTS FOR MODEL WITH AIR BEHIND THE PLATE AT 70 µs.

3.1 Pulse echo on plate

A set of results from the pulse echo experiment is presented in Fig. 5. The recorded echo waveforms for each element are shown in Fig. 5a as logarithmic scaled amplitudes, coding the sign of the waveform with white as positive and black as negative. One can observe that the experimental result shows the same trends as the simulation (Fig. 4b). In the simulation result we observe that the wavefront of the initial pulse is slightly curved and was measured to have an angle of 9.9°, in agreement with a wave reflected from a surface with a 5° angle. The reverberation train has an angle of 6.3°, hence slightly higher than the 5° tilt of the plate. In the presented measurement example we transmitted from an 8-element aperture, elements 13–20. The electronic transmit steering is set to $\alpha = 10°$. We observe the maximum of

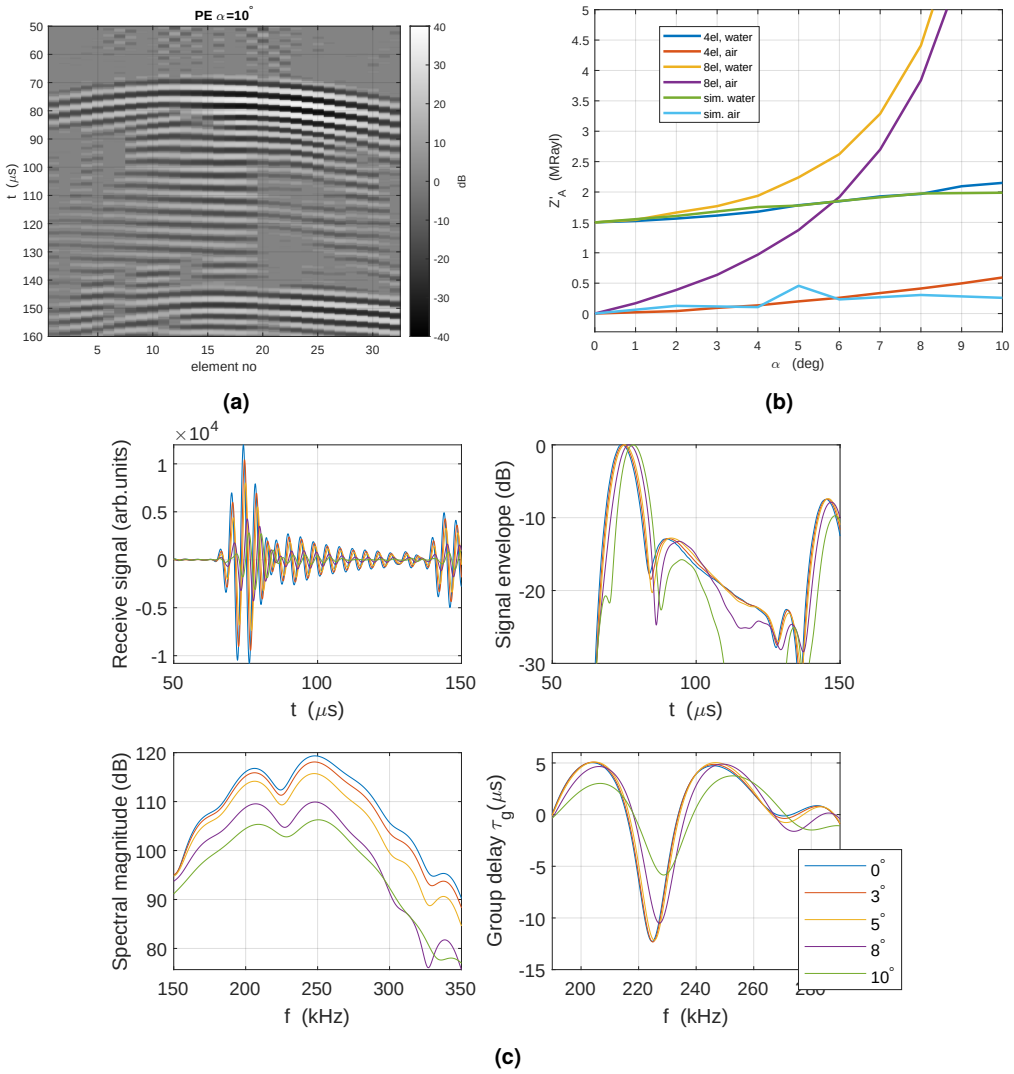

FIGURE 5: EXPERIMENTAL RESULT FROM PERFORMING A PULSE ECHO MEASUREMENT ON PLATE. A) RECORDED RAW DATA AT 32 ELEMENTS. B) APPARENT ACOUSTIC IMPEDANCE AS FUNCTION OF SIMULATED TILT ANGLES. C) EXAMPLE WAVEFORMS, WAVEFORM ENVELOPE, SPECTRUM, AND GROUP DELAY FOR A SET OF SIMULATED TILT ANGLES.

the first echo at elements 20–25 due to the specular reflections from the plate surface, while the reverberation contribution from the plate following the main echo has a lower tilt. Here, we measured the phase front to be approximately 2.5°. Due to the experimental setup beam steering needs to be applied as well to the receiving signal, which results in a 12.5° angle for the received reverberation after this correction. Waveforms derived after beamforming for a set of different tilt angles are shown in Fig. 5c. Clear difference in the amplitudes can be observed for the specular reflection as well as the reverberations for the 5 tilt angles. The envelope of the time signals shows higher attenuation for the ringdown with tilts larger than 5°. This is reflected in the spectrum and the group delay curves where we observe a less pronounced minima for both 8° and 10° tilt angle compared to the results a tilt ≤5°. At the same time we observe a shift in the resonance frequency (location of group delay minimum) for tilt angles larger than 5°.

We have processed the waveforms similarly to the T^3 processing algorithm [2, 29] to derive the estimated impedance Z_A behind the plate (Fig. 5b) from the group delay curve of the measured signals. We have modified this impedance using a linear trend as in [2], normalised to the values for air and water with normal incidence, respectively. This is a fair first approximation according to our experience. One can observe that for the small 4-element aperture, Z_A increases slowly with increasing tilt angle α with a maximum of 0.7 MRayl at 10°. For the larger 8-element aperture, the estimated impedance Z_A for water has increased by 0.5 MRayl at $\alpha = 4.5°$, and for air at $\alpha = 2.5°$. In both cases, the impedance increases significantly with larger tilt angles.

3.2 Pitch catch on plate

For the analysis of the results of the pitch catch example on the plate, we chose to use the furthest of the two positions of the receiving array and an 8-element aperture for transmitting beams. To study the dispersion, we performed a 2D FFT of the waveforms and present the results in the frequency-wavenumber

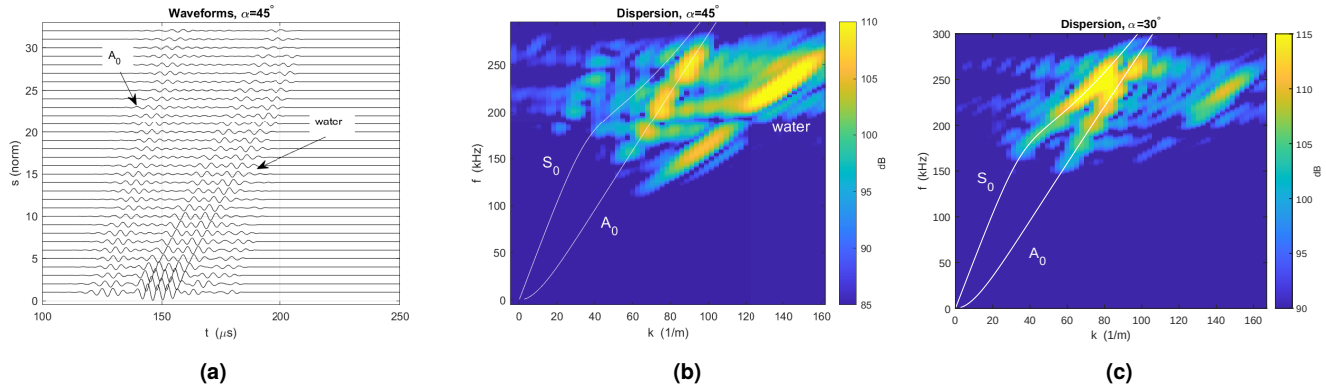

(a) (b) (c)

FIGURE 6: EXPERIMENTAL RESULTS FROM PERFORMING A PITCH-CATCH MEASUREMENT ON A PLATE. A) RECORDED ECHOES ON THE RECEIVING ARRAY WITH AIR BEHIND THE PLATE AND AN 8-ELEMENT TRANSMIT APERTURE B) f-k PLOT FOR $\alpha = 45°$ C) f-k PLOT FOR $\alpha = 30°$.

(f-k) domain as in Fig. 6. The spatial sampling is 3 mm, giving a Nyquist wavenumber of $(1/3\,\text{mm})/2 = 166.7\,1/\text{m}$. The spectra are obtained by zero padding with a factor four in the spatial direction. The waveforms were time gated to 75 µs after first arrival to each element.

The waveforms for the case with a steering angle of 45° are shown in Fig. 6a, where the arrival of the A_0 wave, and the waterborne wave can be observed. The corresponding dispersion diagram is shown in Fig. 6b, where the waterborne and A_0 waves are dominating. The case with a steering angle of 30° is shown in Fig. 6c. For this case, both A_0 and S_0 are apparent, and will co-propagate. Inspection of the waves in the time-space domain (not shown) for this case shows that there is some overlap between the waves, although the S_0 waves lag and are elongated. One may enhance the A_0 wave by beamforming the data on the receiving aperture, corresponding to tilting the aperture by 32°, to fit the A_0 wavefronts' radiation angle given by the mode's phase speed.

The example shows that one has to be careful with the choice of frequency, aperture size, and tilt angle when performing pitch catch experiments. In this case we have a 12.1 mm-steel plate for which the dispersion curves of A_0 and S_0 are close for frequencies around 250 kHz. In order to enhance A_0 and suppress S_0, we had to use a rather high tilt angle $\alpha = 40°$–$45°$. This angle is higher than the optimal angle for coincidence between incoming wave and A_0, which is closer to $\alpha = 32°$–$35°$. It can also be mentioned that when performing electronic beam steering, the effective aperture is the real aperture size projected onto the normal of the beamsteering direction, i.e., scaled with a factor $\cos\alpha$. Thus, the effective transmit aperture will be $8 \cdot 3\,\text{mm}\cos\alpha$, which is 20.8 mm for $\alpha = 30°$ and 17.0 mm for $\alpha = 45°$. This is substantially narrower than the original 24 mm aperture, and will result in a wider beam.

3.3 Guided wave excitation inside of pipe experiment

Figure 7a depicts the f-k plot of the raw recorded data without any filtering or time-gating. The original raw data is similar to the data shown in Fig. 7b and consists of the horizontal union of the individual receiver measurements. However, the data in Fig. 7b is filtered to remove noise and increase readability. Three waves are visible in the f-k plot: the guided waves belonging to the A_0 and S_0 modes, and the direct water wave. These two excited waves can, at a future stage, be analysed to determine the properties of the material behind the inner pipe.

The filtered data in time domain of Fig. 7b allows analysing one of the observed guided waves in Fig. 7a. The A_0 wave arrives at approx. 100 μs and travels along the pipe. However, there are numerous reverberations of the same type. One reason for this is, that the guided wave propagates along the pipe and also leaks energy into the cavity between the pipes. This wave gets reflected at the outer pipe and excites another guided wave inside the inner pipe. Many more such pathways can be envisioned and they are due to the numerous reverberations that can take place as waves get reflected at the different interfaces. Future research will focus on extracting information from this part of the signal and a main objective is to extract information on the state of material, such as a bonded or de-bonded cement, at the outer surface of the second (outer) pipe.

4. CONCLUSIONS

This paper presents results on pulse-echo and pitch-catch experiments performed with ultrasonic phased arrays. Experiments are performed on a flat steel plate and inside a pipe setup similar to the geometries encountered in borehole applications. This is the first use of this set of ultrasonic phased arrays that are specifically designed for applications in well logging, i.e. their centre frequencies are tailored to the thickness of pipes encountered in the field. The phased arrays are controlled with an ultrasonic scanner in a fashion similar to medical ultrasound imaging, i.e. signals from all individual elements are recorded in parallel and beam-steering is conducted by prescribing delays electronically.

The pulse-echo experiment on a flat plate was compared with numerical simulations. Here, we reproduced the well-known result that the estimated acoustic impedance is affected by misalignment of the transducer. For a realistic size of the transducer, 24 mm, we observed substantial overestimation of Z_A when $\alpha > 5°$. It was also observed in both simulations and experiments that the reverberation part of the echo had a tendency towards lower misalignment than the specular part of the signal. The smaller aperture, with its wider beam, reduced the effect of

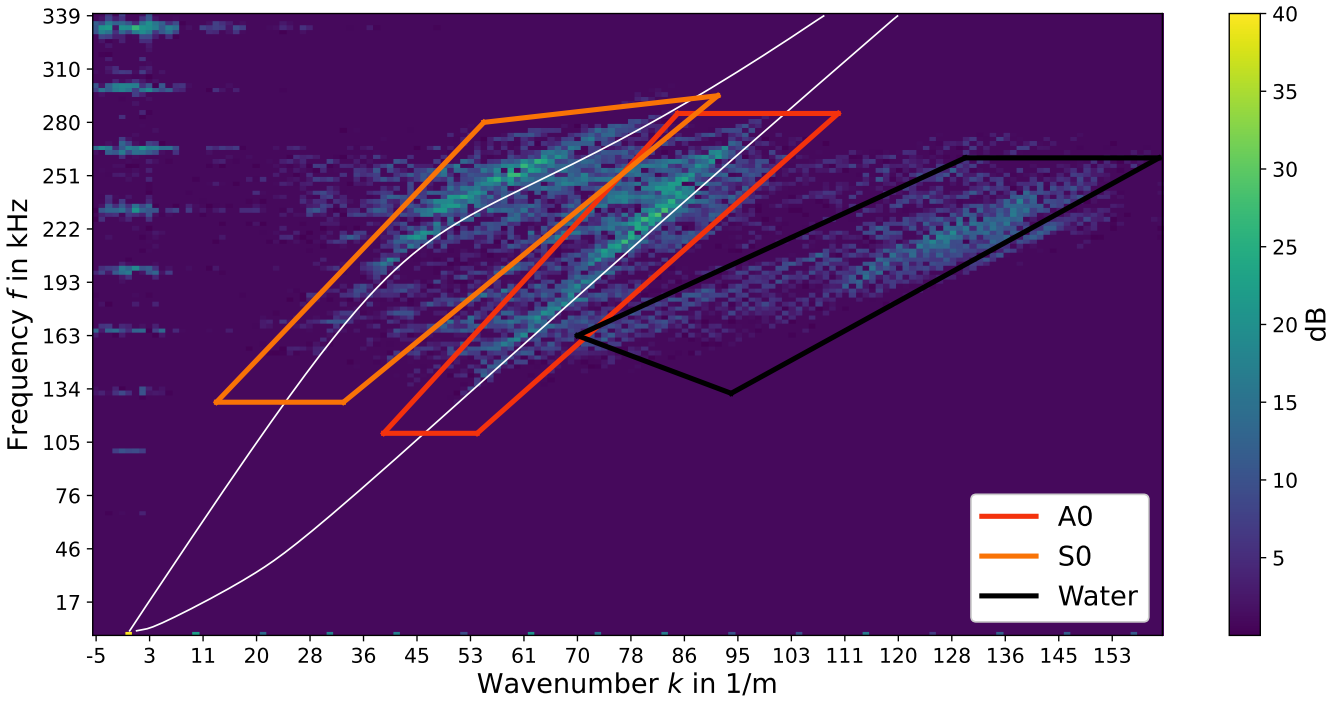

(a)

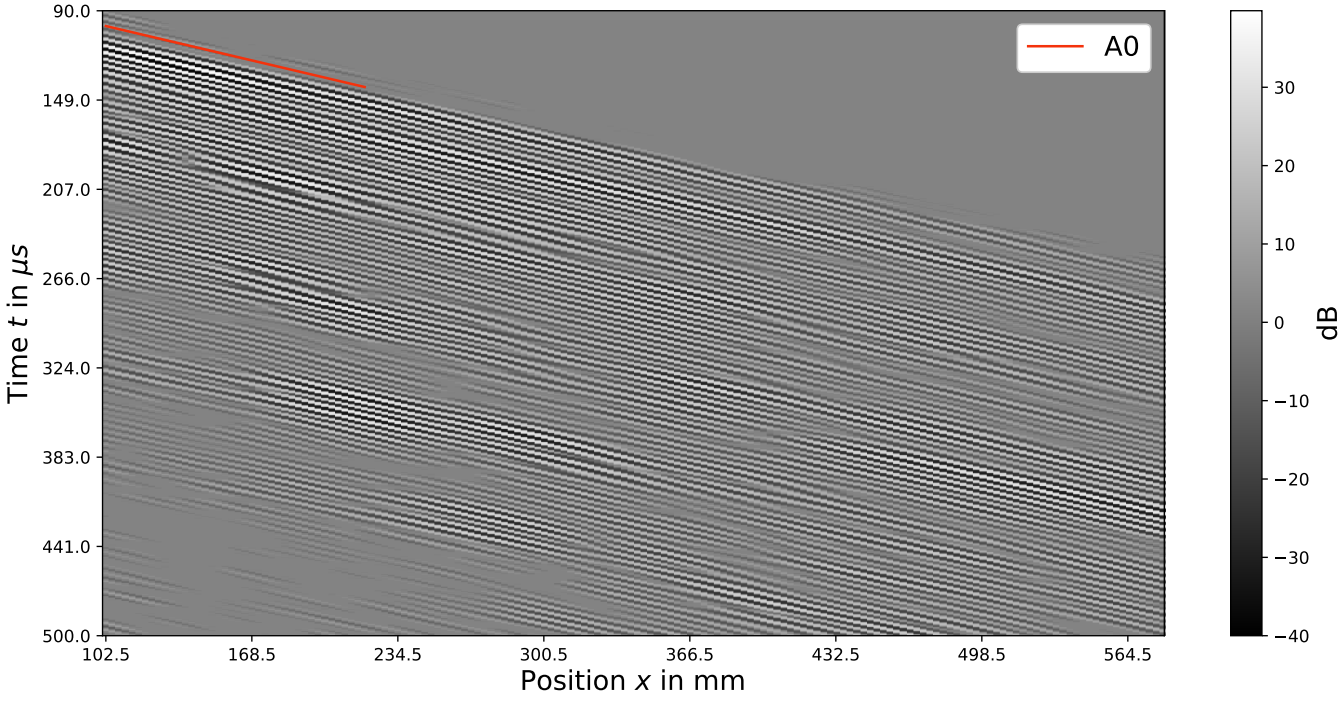

(b)

FIGURE 7: EXPERIMENTAL RESULT FROM A PITCH-CATCH MEASUREMENT IN THE PIPE EXPERIMENT. A) FREQUENCY-WAVENUMBER DEPICTION OF THE RECORDED DATA FROM A PITCH-CATCH EXPERIMENT. THREE WAVES ARE VISIBLE: A_0, S_0 AND THE WATERBORNE WAVE. THE OBSERVED SLOPES MATCH WITH THEORETICAL RESULTS ON THE DISPERSION RELATION (DEPICTED IN WHITE). B) RECORDED DATA AFTER FILTERING BY ONLY KEEPING COMPONENTS OF THE A_0 MODE. DATA IS ONLY SHOWN FOR HALF OF THE RECORDED AXIAL LENGTH BECAUSE THE SIGNAL IS WEAK FOR HIGHER VALUES OF x. A TIME-GATING IS CONDUCTED TO REMOVE NOISE PRIOR TO THE ARRIVAL OF THE FIRST SIGNAL. FILTERING IS CONDUCTED BY ZEROING DATA OUTSIDE OF THE A_0 BOX IN A) AND PERFORMING AN INVERSE FOURIER TRANSFORMATION.

the misalignment of the transducer. For the pitch-catch measurement on the same plate we studied how different plate modes were excited and propagated as function of angle of incidence. We demonstrated how other modes than the desired A_0 mode could be suppressed, and that the waveform of interest could be emphasised by electronic tilting of the receiving aperture. Finally, the pitch-catch functionality was tested inside a setup with two concentric pipes. By using arrays, guided waves inside the innermost pipe can be recorded quickly over a large axial distance.

The results in this paper demonstrate the high flexibility that phased arrays offer for applications in well logging. Control of the ultrasonic waves and parallel recording allow implementing new methods. The work in this paper is a first step in commissioning the arrays and the laboratory by operating them in the well-established pulse-echo and pitch-catch mode. Future work will focus on using the laboratory to implement more advanced imaging algorithms and to interrogate the reverberations in the pitch-catch signal to determine if parts can be identified that reveal information beyond the outside of the second pipe.

ACKNOWLEDGEMENTS

The research in this paper has been funded by the Research Council of Norway (RCN) under the project *Norwegian P&A Laboratories* (RCN grant no. 296009). T.F.J. and E.M.V. also gratefully acknowledge funding from the RCN via the Centre for Innovative Ultrasound Solutions (RCN grant no. 237887).

REFERENCES

[1] Allouche, Mickael, Guillot, Dominique, Hayman, Andrew J., Butsch, Robert J. and Morris, Charles W. "Cement Job Evaluation." Nelson, Erik B. and Guillot, Dominique (eds.). *Well Cementing*, 2nd ed. Schlumberger (2006): Chap. 15, pp. 549–612.

[2] Hayman, Andrew J., Hutin, Remi and Wright, Peter V. "High-Resolution Cementation and Corrosion Imaging by Ultrasound." *SPWLA 32nd Annual Logging Symposium*: p. 25. 1991.

[3] van Kuijk, Robert, Zeroug, Smaine, Froelich, Benoit, Allouche, Michael, Bose, Sandip, Miller, Douglas, le Calvez, Jean-Luc, Schoepf, Virginie and Pagnin, Andrea. "A Novel Ultrasonic Cased-Hole Imager for Enhanced Cement Evaluation." *International Petroleum Technology Conference*: p. 14. 2005. DOI 10.2523/IPTC-10546-MS.

[4] Haldorsen, Jakob B. U., Stensrud, Espen, Merciu, Ioan-Alexandru and Miller, Douglas E. "Characterizing borehole plumbing using full-waveform ultrasonic data: Application to data from a North Sea well." *Geophysics* Vol. 81 No. 6 (2016): pp. B189–B199.

[5] Haldorsen, Jakob B. U., Stensrud, Espen, Merciu, Ioan-Alexandru and Miller, Douglas E. "Decomposing full-waveform borehole acoustic data with application to data from a North Sea well." *Geophysics* Vol. 81 No. 4 (2016): pp. IM71–IM95.

[6] Cheeke, J. David N. *Fundamentals and applications of ultrasonic waves*. CRC press (2010).

[7] Franconi, Nicholas G., Bunger, Andrew P., Sejdić, Ervin and Mickle, Marlin H. "Wireless communication in oil and gas wells." *Energy Technology* Vol. 2 No. 12 (2014): pp. 996–1005.

[8] Jensen, Jørgen A. "Medical ultrasound imaging." *Progress in biophysics and molecular biology* Vol. 93 No. 1-3 (2007): pp. 153–165.

[9] Chen, Xiaozhao, Bao, Nan, Li, Jianhua and Kang, Yan. "A review of surgery navigation system based on ultrasound guidance." *2012 IEEE International Conference on Information and Automation*: pp. 882–886. 2012. IEEE.

[10] Mason, Timothy J. "Therapeutic ultrasound an overview." *Ultrasonics sonochemistry* Vol. 18 No. 4 (2011): pp. 847–852.

[11] Von Ramm, Olaf T. and Smith, Stephen W. "Beam steering with linear arrays." *IEEE transactions on biomedical engineering* No. 8 (1983): pp. 438–452.

[12] Thomenius, Kai E. "Evolution of ultrasound beamformers." *1996 IEEE Ultrasonics Symposium. Proceedings*, Vol. 2: pp. 1615–1622. 1996. IEEE.

[13] Jensen, Jørgen A., Nikolov, Svetoslav I., Gammelmark, Kim L. and Pedersen, Morten H. "Synthetic aperture ultrasound imaging." *Ultrasonics* Vol. 44 (2006): pp. e5–e15.

[14] Holmes, Caroline, Drinkwater, Bruce W. and Wilcox, Paul D. "Post-processing of the full matrix of ultrasonic transmit–receive array data for non-destructive evaluation." *NDT & E International* Vol. 38 No. 8 (2005): pp. 701–711.

[15] Drinkwater, Bruce W. and Wilcox, Paul D. "Ultrasonic arrays for non-destructive evaluation: A review." *NDT & E International* Vol. 39 No. 7 (2006): pp. 525–541.

[16] Zhang, Jie, Drinkwater, Bruce W., Wilcox, Paul D. and Hunter, Alan J. "Defect detection using ultrasonic arrays: The multi-mode total focusing method." *NDT & E International* Vol. 43 No. 2 (2010): pp. 123–133.

[17] NorPALabs. "Norwegian P&A Laboratories – NorPALabs." (2020). Accessed 9 January 2023, URL https://norpalabs.no/.

[18] Vrålstad, Torbjørn, Saasen, Arild, Fjær, Erling, Øia, Thomas, Ytrehus, Jan David and Khalifeh, Mahmoud. "Plug & Abandonment of Offshore Wells: Ensuring Long-Term Well Integrity and Cost-Efficiency." *Journal of Petroleum Science and Engineering* Vol. 173 (2019): pp. 478–491. DOI 10.1016/j.petrol.2018.10.049.

[19] Khalifeh, Mahmoud and Saasen, Arild. *Introduction to permanent plug and abandonment of wells*. Springer Nature (2020).

[20] Klieber, Christoph, Brill, Thilo M., Catheline, Sebastien, Vincensini, Y. and Mege, Fabrice. "Visualization of Leaky Ultrasonic Lamb Wave Experiments in Multilayer Structures." *Physics Procedia* Vol. 70 (2015): pp. 314–317. DOI 10.1016/j.phpro.2015.08.162.

[21] Talberg, Andreas S. "Experimental evaluation of broadband wave propagation in plates." Master's Thesis, NTNU. 2016.

[22] Viggen, Erlend M., Johansen, Tonni F. and Merciu, Ioan-Alexandru. "Simulation and modeling of ultrasonic pitch-catch through-tubing logging." *Geophysics* Vol. 81 No. 4 (2016): pp. D383–D393.

[23] Viggen, Erlend M., Johansen, Tonni F. and Merciu, Ioan-Alexandru. "Simulation and inversion of ultrasonic pitch-catch through-tubing well logging with an array of receivers." *NDT & E International* Vol. 85 (2017): pp. 72–75.

[24] Arnestad, Håvard K. "A Fast Simulation Method for Ultrasonic Wave Propagation in Coupled Non-Parallel Plates — with Applications to Inversion of Pitch-Catch Through-Tubing Well Logging." Master's Thesis, Norwegian University of Science and Technology, Trondheim. 2021.

[25] Junqueira, Bernardo F., Leiderman, Ricardo and Castello, Daniel A. "An Analytical–Numerical Formulation to Modelling Wave Propagation in Double-Cased Oil Wells." *Wave Motion* Vol. 112 (2022): p. 102942. DOI 10.1016/j.wavemoti.2022.102942.

[26] Bose, Sandip, Zhu, Lingchen, Zeroug, Smaine, Merciu, Ioan Alexandru, Constable, Kevin, Hemmingsen, Pål V., Berg, Eirik, Wielemaker, Erik, Govil, Amit and Kalyanaraman, Ram S. "Acoustic Evaluation of Annulus B Barriers Through Tubing for Plug and Abandonment Job Planning." *Proceedings of the Offshore Technology Conference*: p. D031S035R005. 2021. OTC, Virtual and Houston, Texas. DOI 10.4043/31302-MS.

[27] Wooh, Shi-Chang and Shi, Yijun. "Optimum beam steering of linear phased arrays." *Wave motion* Vol. 29 No. 3 (1999): pp. 245–265.

[28] Huber, Armin. "The Dispersion Calculator: An open source software for calculating dispersion curves and mode shapes of guided waves." DLR Center for Lightweight Production Technology (2018). Accessed 9 January, 2023, URL https://www.dlr.de/zlp/en/desktopdefault.aspx/tabid-14332/24874_read-61142/.

[29] Wright, Peter. "Method and Apparatus for the Acoustic Investigation of a Casing Cemented in a Borehole." (1993). US Patent 5,216,638.